HHS Public Access

Author manuscript

Magn Reson Imaging. Author manuscript; available in PMC 2016 December 01.

Published in final edited form as:

Magn Reson Imaging. 2015 December ; 33(10): 1267–1273. doi:10.1016/j.mri.2015.08.006.

Diffusion MRI with Semi-Automated Segmentation Can Serve as a Restricted Predictive Biomarker of the Therapeutic Response of Liver Metastasis

Renu M. Stephen[1], **Abhinav K. Jha**[2], **Denise J. Roe**[1,3], **Theodore P. Trouard**[4,5], **Jean-Philippe Galons**[5], **Matthew A. Kupinski**[2,5], **Georgette Frey**[1], **Haiyan Cui**[1], **Scott Squire**[5], **Mark D. Pagel**[1,4,5,6], **Jeffrey J. Rodriguez**[7], **Robert J. Gillies**[8], and **Alison T. Stopeck**[1]

[1]University of Arizona Cancer Center, University of Arizona, Tucson, AZ

[2]College of Optical Sciences, University of Arizona, Tucson, AZ

[3]Mel and Enid Zuckerman College of Public Health, University of Arizona, Tucson, AZ

[4]Department of Biomedical Engineering, University of Arizona, Tucson, AZ

[5]Department of Medical Imaging, University of Arizona, Tucson, AZ

[6]Department of Chemistry and Biochemistry, University of Arizona, Tucson, AZ

[7]Electrical and Computer Engineering, University of Arizona, Tucson, AZ

[8]H. Lee Moffitt Cancer Center and Research Institute, Tampa, FL

Abstract

Purpose—To assess the value of semi-automated segmentation applied to diffusion MRI for predicting the therapeutic response of liver metastasis.

Methods—Conventional diffusion weighted magnetic resonance imaging (MRI) was performed using b-values of 0, 150, 300 and 450 s/mm^2 at baseline and days 4, 11 and 39 following initiation of a new chemotherapy regimen in a pilot study with 18 women with 37 liver metastases from primary breast cancer. A semi-automated segmentation approach was used to identify liver metastases. Linear regression analysis was used to assess the relationship between baseline values of the apparent diffusion coefficient (ADC) and change in tumor size by day 39.

Results—A semi-automated segmentation scheme was critical for obtaining the most reliable ADC measurements. A statistically significant relationship between baseline ADC values and change in tumor size at day 39 was observed for minimally treated patients with metastatic liver lesions measuring 2–5 cm in size ($p = 0.002$), but not for heavily treated patients with the same tumor size range ($p = 0.29$), or for tumors of smaller or larger sizes. ROC analysis identified a

Corresponding Author: Renu M. Stephen, rstephen1@gmail.com, Address: University of Arizona Cancer Center, University of Arizona, 1515 N. Campbell Avenue, P.O. Box 245024, Tucson, AZ 85724, Phone: (520) 626-8557, Fax: (520) 626-5051.

baseline threshold ADC value of 1.33 μm^2/ms as 75% sensitive and 83% specific for identifying non-responding metastases in minimally treated patients with 2–5 cm liver lesions.

Conclusion—Quantitative imaging can substantially benefit from a semi-automated segmentation scheme. Quantitative diffusion MRI results can be predictive of therapeutic outcome in selected patients with liver metastases, but not for all liver metastases, and therefore should be considered to be a restricted biomarker.

Keywords

Liver imaging; diffusion MRI; restricted biomarker; breast cancer

Introduction

Diffusion-weighted magnetic resonance imaging (DW-MRI) is sensitive to the microscopic random motion of water molecules, which can be quantified via the apparent diffusion coefficient (ADC) [1]. The ADC provides quantitative information regarding the cellularity and cell membrane integrity of biologic tissue. The initial average ADC value has been shown to predict tumor response to therapy [2,3]. For example, DW-MRI has been used to measure therapy response during pre-clinical [4–10] and clinical studies of primary brain cancer [11–13], colorectal cancer [14–17], osteosarcomas [18,19] and breast cancer [20–22]. Moreover, the use of non-ionizing radiation as well as the short time and ease of acquisition permit longitudinal information to be safely collected, which are attractive features for clinical assessments of cancer.

ADC values measured prior to initiating treatment have been shown to potentially predict treatment response [23] and disease survival [24] in colorectal cancer patients with liver metastases. However, measuring the ADC value of a liver lesion is technically challenging, because diffusional motion in a liver lesion is confounded by non-rigid body visceral motion due to respiration, cardiac motion, blood flow and motility [25,26]. These confounding factors may be eliminated or mitigated by using advanced postprocessing methods that improve the identification of lesion borders and the quantitative estimation and evaluation of ADC values. Furthermore, the manual evaluation of large volumes of DW-MR images can be a daunting challenge in a radiology clinic. Therefore, a primary aim of this study was to develop a robust post-processing protocol for obtaining reliable results from DW-MRI of liver metastases, by evaluating the merits of automatic and semi-automatic lesion segmentation relative to manual segmentation.

Previous DW-MRI studies of liver metastases have evaluated patients with specific conditions [23,24]. Patients enrolled in these studies were undergoing their first chemotherapy treatment regimen, and had a minimum number of liver lesions. The DW-MRI analyses were restricted to lesions in specific liver lobes and morphologic locations, and to lesions that were greater than 1 or 1.6 cm in diameter. These criteria for patient enrollment and for selecting liver lesions for analyses suggest that DW-MRI may only apply as a “restricted” predictive biomarker, known as a biomarker for predicting treatment response under restricted conditions. Therefore, another primary aim of our study was to evaluate whether DW-MRI can serve as a robust biomarker for all patients with all sizes of

liver metastases in all liver locations, or whether DW-MRI should be used as a restricted biomarker for assessing liver metastases. To investigate this aim, we conducted a pilot clinical trial in breast cancer patients with known liver metastases.

Materials and Methods

Patients

Twenty-eight women with metastatic breast cancer and liver metastases were recruited from the breast cancer clinics of the University of Arizona Cancer Center. All patients provided informed written consent, had a minimum of one liver metastasis measurable over 1.2 cm in at least two dimensions, were not pregnant, at least 18 years of age and scheduled to initiate a new chemotherapy regimen for their metastatic disease. Metastatic lesions were identified by a radiologist using computed tomography (CT) or conventional MRI. Patients were divided into two categories based on their prior number of chemotherapy regimens in the metastatic setting. The minimally treated group included only those patients receiving first-line chemotherapy or who had progressed on a single prior chemotherapy regimen for their metastatic disease (second line). Heavily treated patients were defined as having received two or more prior chemotherapy regimens for their metastatic disease. Prior hormonal and adjuvant therapies were excluded for determining the number of prior chemotherapy regimens. All patients underwent MRI examinations at baseline and again at 4, 11 and 39 days after initiating a new chemotherapy regimen. Up to three liver lesions were measured in each patient for a total of 37 liver metastases analyzed. The protocol was approved by the university's institutional review board and conducted in accordance with the Health Insurance Portability and Accountability Act.

MRI

All imaging was carried out on a 1.5 T Signa LXi Excite MRI scanner using the body radiofrequency (RF) coil for excitation and an 8-channel phased array RF coil for reception (General Electric Medical Systems, Waukeshaw, WI). Following a standard localization sequence, T1-weighted and diffusion-weighted imaging of the entire liver were carried out in the axial plane. T1-weighted imaging employed a dual-echo spoiled gradient recalled echo (SPGR) during breath-hold and was acquired with TE1=2.0 ms, TE2=4.3 ms, TR=160 ms, FA=90°, BW=±62.5 kHz, FOV=38×38 cm^2, slice thickness=8 mm contiguous, matrix=256×160 and number of excitations (NEX, averages)=1 with 5 cm thick spatial saturation bands applied immediately superior and inferior to the imaging volume. A three-dimensional fat-suppressed SPGR was also acquired using TE=1.9 ms, TR=6 ms, TI=40 ms, FA=15°, BW=±31.2 kHz, FOV=38×38 cm^2, slice thickness=6 mm, matrix=256×128 and NEX=1.

Axial diffusion-weighted images were acquired within a 24-second breath-hold on inspiration using a single-shot echo-planar sequence with the following parameters: TE=91.6 ms, TR=6000 ms, BW=±125 kHz, FOV=38×38 cm^2, slice thickness=6 mm contiguous, matrix=128×128 and NEX=1. During each breath-hold, four diffusion-weighted images were acquired, including one image with b=0 s/mm^2 (no diffusion weighting) and with b=150, 300, or 450 s/mm^2. Larger b-values were not used in this study to maintain

good signal sensitivity in DW-MR images. For DW-MRI at each b-value, three images were acquired with diffusion weighting applied along the read, phase and slice direction. The effect of anisotropic diffusion was reduced by averaging the signal from the three orthogonal directions of diffusion weighting.

Analysis

MR images were retrospectively reviewed in a random manner by a board-certified MR radiologist who provided bi-dimensional measurements. The reviewer was blinded to the therapeutic response and the ADC measurements of the lesions.

Manual segmentation of liver lesions can be difficult, time consuming and error-prone due to several reasons, including irregular and/or indistinct lesion boundaries, low signal-to-noise ratio, wide intensity and morphological variations of the lesion, and the large number of images that must be analyzed. Further, the lesion could also have exhibited movement across the different b values. In order to improve the speed, accuracy and reliability of DW-MRI analysis, a computer program for automated image analysis was developed for both lesion segmentation and ADC estimation. Details of the methods used in this program are presented elsewhere [27–31] and, for brevity, are only summarized here. The automated analysis is carried out in several steps. A given lesion was spread across multiple slices. In the algorithm initialization step, using the radiologist's annotation of the T1-weighted images as a guide, the analyst drew a large rectangular region of interest (ROI) on one of the images such that the lesion was within this ROI in all the images that contained the lesion for all the b values. Following this, a pixel that lay within the lesion region was marked as the seed pixel. This initialization of drawing the ROI and identifying a seed pixel was performed only once for a given set of patient images. Subsequently, the program processed all the slices containing the lesion for each b value. For each slice, the algorithm considered the histogram of the pixel intensities inside the ROI as a finite Gaussian mixture (FGM) model. To account for spatial information, each region in the image was modeled as a Markov random field (MRF) and characterized by a Gibbs distribution. Using these two statistical models, the lesion within the ROI was segmented for each slice. The algorithm also took into account the geometrical constraint of convexity of the lesion to improve the accuracy of segmentation, especially when the lesion region was surrounded by regions that had pixel intensities similar to that of the lesion. The segmented lesion in each slice was displayed to the diffusion analyst. We have independently studied the performance of this segmentation algorithm using the standard evaluation method of comparing the performance of this algorithm with results from a carefully performed manual segmentation [27]. Further, we have also independently and objectively evaluated this algorithm based on how well it aids in the task of ADC estimation [32]. Our studies indicate that this algorithm is accurate and reproducible both with standard [27] and task-based evaluation methods [32], and also outperforms several commonly used segmentation techniques. However, there were a few instances when the automated segmentation failed when there was a second lesion or another anatomical structure near the lesion of interest. For example, the segmentation was outside the bounding box, the segmented region had sub regions of very different intensities, or the segmented contour had a completely irregular shape consisting of multiple intersecting regions. Thus, to ensure an even higher segmentation success rate, the analyst

had the option to perform minor modifications to the segmentation (known as semi-automated segmentation), or manually segment the lesion in the particular slice (manual segmentation). Using this method, the segmented lesion was obtained for all the b values. The performances of these automated, semi-automated, and manual methods were compared to evaluate the reliability and accuracy of the ADC value estimated using each of these segmentation procedures. An analysis method was considered to be reliable when the fitting of DW-MRI signal amplitudes produced ADC values with low variance, and produced results that were within the range of typical physiological ADC values.

The next task was to estimate the ADC of the lesion from these segmented lesions. One approach could be to estimate the ADC of each lesion pixel, and thus create an ADC map of the lesion. However, the liver exhibits visceral motion across the different b values leading to mis-registration of the images at the different b values [20]. Therefore, a pixel wise analysis approach would result in errors that would depend on the amount and type of motion, and the composition of the tumor. The error would be severe for tumors that are very heterogeneous. Thus, instead of taking this approach, we computed the mean signal intensity of the lesion at the different b values, which is relatively invariant to lesion movement. Then the program estimated the ADC value of the lesion using a maximum-likelihood (ML) method that accounts for the statistics of the lesion mean signal intensity. The ML method computed the ADC value that maximizes the probability of occurrence of the measured mean signal intensity values [28,29,31]. The performance of this ML method has been previously investigated using independent simulation studies. In these studies, the size, signal-to-noise-ratio (SNR) and true ADC value of the lesion was varied. Across all the variations, it was observed that the ML method was accurate, reliable, and outperformed the conventional linear-regression based method for ADC estimation.

Several variables that may affect the ability of the ADC to predict clinical responses were examined. The automated segmentation and ADC estimation algorithms were used to evaluate the choice of b-value pairs (b = 0 paired with, sequentially, b = 150, b = 300 and b = 450 s/mm^2). Fully automated, semi-automated and manual segmentation were used to evaluate a single center slice compared to multiple slices containing the lesion of interest. Because the edges of lesions may be affected by tissue edema, the proportion of region considered within each segmented lesion was altered, and the ADC values obtained from progressively smaller areas of the lesion were compared. An erosion-based algorithm [32,33] was combined with the automated segmentation algorithm, resulting in different ROIs for analysis. ROIs representing 90, 80 and 65 percent of the total estimated lesion size were used to calculate the ADC and determine if ADC values from smaller fractions of the total ROI would better predict clinical responses. Baseline lesion size (<2cm, 2–5cm or >5cm), baseline ADC value, and prior treatments (minimally versus heavily treated) were independently examined as predictors of clinical response.

Statistical Analysis

We used a linear mixed-effects model to statistically compare the ADC values obtained using the three b-value pairs (b0–b150, b0–b300, b0–b450), segmentation methods (manual, fully automated, semi-automated), number of slices (single versus multiple), and

progressively smaller proportions of the segmented lesion (100%, 90%, 80%, 65%). Patients were considered a random effect while the imaging characteristics were considered fixed effects. Reliability was defined as the patient variance divided by the total variance. Tukey's studentized range test was used to assess the significance of pairwise differences between the groups adjusted for multiple comparisons. A statistically significant difference was considered evidence for non-comparability of methods.

The change in tumor size was calculated as the ratio of the tumor size at day 39 divided by the baseline tumor size. Tumor response was dichotomized as a responder if the reduction in tumor size at day 39 was > 1 cm and a non-responder if the change was ≤ 1 cm. All statistical models were adjusted for prior therapies (minimally versus heavily treated), an established predictor of tumor responsiveness. Median time to progression was estimated using the Kaplan-Meier estimate. The statistical significance of the difference in time to progression was tested using the log-rank test. Linear regression analysis was used to assess the relationship between the change in tumor size versus baseline ADC (using a robust variance estimate due to multiple lesions within the same patient). Because the relationship was statistically significant only for those minimally treated (i.e., there was a statistically significant interaction), subsequent models assessed the relationship separately for those minimally versus heavily treated. Logistic regression analysis was used to determine an optimal cut-point to predict response for those minimally treated (with a robust variance estimate). The receiver operating characteristic (ROC) was computed using a curve of sensitivity versus 1-specificity across multiple cut-points of the ADC values. The ADC cut-point was selected as the value that resulted in the greatest sum of sensitivity and specificity, i.e. the value that maximizes Youden's index.

Results

Patient Characteristics

Of the 28 patients that consented, 18 patients had evaluable data and ten patients were excluded from the analysis (Table 1). One patient had inadequate MR image quality resulting from motion-induced artifacts, five patients contained diffuse liver lesions that could not be reliably measured, one patient had a complete response, one patient expired prior to day 39, and two patients signed consent forms but did not enter the study. The mean age was 52 years, with a range from 30 to 82 years. Approximately 44% of the patients were minimally treated and 55% were heavily treated. The average lesion size was 2.32 and 3.09 cm for minimally treated patients and heavily treated patients, respectively, which were not statistically different ($p > 0.25$).

MRI Results

As shown by representative MR images of a minimally treated patient, metastatic lesions were visible as a hypointense region in the T1-weighted image and as a hyperintense region on the corresponding DW images (Figure 1). In general, breath-holding techniques allowed for acceptable images that were individually free from motion-related artifacts. The mean signal intensities obtained from the lesions at different b-values were used to compute a global ADC value (Figure 2).

ADC values generated from three b-value pairs (b0–b150, b0–b300 and b0–b450) were compared at all imaging time points (baseline, day 4, day 11 and day 39). The b0–b300 and b0–b450 pairs yielded comparable ADC results, as demonstrated by the lack of statistically significant differences in the observed values (Table 2). The standard errors associated with the ADC values calculated from the b0–b450 pair were consistently lower compared to the other pairs, and thus the b0–b450 pair was chosen as the most robust pair for all subsequent analyses.

To investigate the scope of imaging results that must be analyzed for adequately assessing the ADC values of liver lesions, we compared the results from analyzing a single imaging slice vs. multiple slices. There was no statistical difference between analyzing multiple slices of the lesion versus a single central slice to calculate the ADC values using segmentation methods that were fully automated ($p=0.463$), fully manual ($p=0.748$) and semi-automated ($p=0.626$; Table 3). Notably, the analyzed liver lesions were located throughout the liver and were not restricted to specific liver regions or lobes. These results indicated that the ADC values of liver metastases in our pilot study were adequately homogeneous throughout the liver to allow for single-slice analyses, which improved the efficiency of our subsequent image evaluations.

The evaluations of the fully automated, fully manual, and semi-automated segmentation methods revealed that the three methods generated statistically comparable results ($p>0.59$ for all comparisons). In addition, the comparison of smaller regions of interest (ROIs), including 90%, 80% and 65% of a lesion's ROI volume, revealed no significant difference in mean ADC values over any of these analyses (data not shown). This result further substantiated that semi-automated analysis of the tumor region is not affected by potential mis-segmentation that under-represents the tumor volume, and therefore semi-automated segmentation is a robust process for this type of image analysis.

Lesions < 2 cm or > 5 cm were difficult to segment by all methods. In addition, the analysis of smaller and larger legions routinely produced fittings to the DW-MRI signal amplitudes that produced ADC values with a large variance, or produced ADC values that were not within the range of typical physiological ADC values, and therefore were considered to be unreliable. For comparison, lesions measuring 2–5 cm at baseline were relatively straightforward to segment and produced reliable ADC values over the course of the imaging protocol and were preferentially chosen for subsequent analysis. This result indicated that the DW-MRI analysis of liver lesions should be limited to a restricted condition of 2–5 cm lesion diameter.

Predictors of Response

The characteristics of the lesion and patient, including the baseline lesion size, baseline ADC value, and minimal vs. extensive prior treatments, were evaluated as possible predictors of therapy response. Notably, these characteristics were not related, because the baseline ADC values did not correlate with the size of the metastatic lesion or number of prior therapies (Table 4), and the lesion size and number of prior therapies were also uncorrelated. Minimally treated patients had a longer time to progression at 26 weeks

compared to 11 weeks for the heavily treated patients, though this was not statistically significant due to the small sample size of this pilot study (p=0.298). Similarly, the baseline lesion size and therapy response were not correlated.

Most importantly, there was a significant correlation between baseline ADC and change in tumor size between baseline and day 39 for minimally treated patients (p = 0.002), with lesions having a lower ADC value more likely to have a tumor response (Figure 3A). A similar correlation was not observed in lesions from heavily treated patients (p = 0.29) (Figure 3B). For patients with minimal treatment, a Receiver Operating Characteristic (ROC) analysis identified a threshold ADC value of 1.33 $\mu m^2/ms$ as 75% sensitive (6 out of 8) and 83% specific (5 out of 6) for identifying non-responding metastases. Using this ADC value as a cut-point, 79% of the lesions were correctly classified for day 39 tumor response. Therefore, these results indicate that the DW-MRI analysis of liver metastases should be limited to a restricted condition of only assessing minimally treated patients.

For comparison, the change in the ADC value between the baseline measurement and day 4 after initiating treatment did not show a correlation with change in tumor size. Similarly, the changes in ADC between baseline and day 11 were also uncorrelated with a change in tumor size. This lack of a correlation was observed for both minimally treated patients and heavily treated patients. This lack of a correlation may be due to tumor changes that occur during treatment, including cellular swelling, tissue edema, or vascular congestion [34,35].

Discussion

A primary aim of our study was to establish a robust post-processing protocol for obtaining reliable results from DW-MRI of liver metastases. This reliability was evaluated by comparing the assessments of multiple slices or a single center slice of the lesion, which showed that a single-slice analysis was adequate. No significant difference in ADC values was observed between the fully automated, fully manual, and semi-automated segmentation methods. Our results agree with a previous study using manually determined and automatically determined ROIs for evaluating ADC values, which also concluded that a computer-generated segmentation approach can be reliable [36]. We also demonstrated that potentially underestimating the segmented region through an automated or semi-automated segmentation method does not significantly change the ADC value. Overall, these results indicate that considerable time can be saved with a semi-automated, single-slice analyses.

DW-MRI results with low b-values are known to include contributions from perfusion as well as diffusion. Our study included DW-MRI with a b-value of 0 s/mm^2 in our analyses to improve image signal sensitivity, and therefore inherently included some influence from perfusion. Indeed, the inferiority of the ADC values calculated from the b0–b150 pair may be due to perfusion effects typically seen in the low b-value range, which is even greater in vascular rich tissues such as the liver [37]. In addition, the higher ADC values determined from the b0–b150 pair in our study is consistent with other studies that demonstrated elevated ADC values obtained from DW-MRI with low b-value ranges in highly perfused organs [26,38]. For comparison, a previous study found that a perfusion-sensitive evaluation determined with b0–b500 s/mm^2 had elevated ADC values in responding and

nonresponding metastatic liver lesions, but a perfusion-insensitive evaluation determined with b150–b500 s/mm^2 did not have elevated ADC values. Yet the direction of response was similar in both groups [26]. Therefore, our observation that baseline ADC values predict treatment response for minimally-treated patients is not expected to change if other b-values are used in future studies.

Another primary aim of our study was to assess the value of DW-MRI as a robust biomarker for all liver metastases, or as a restricted biomarker for a specific subset of liver metastases. This prospective study examined the influence of baseline lesion size when using ADC values to predict tumor responses to therapy. Historically, baseline liver lesions with diameters ranging between 1.0 and 14.9 cm have been used in predicting response to therapy, and only patients undergoing their first chemotherapeutic treatment regimen have been enrolled in these studies [23,38,39]. However, our study has demonstrated that restricting analyses to lesions with diameters ranging between 2 and 5 cm produced more reliable ADC values. Therefore, the ADC value from DW-MRI studies should be used as a restricted biomarker for assessing liver lesions in this intermediate size range.

This prospective study also examined the influence of the number of prior lines of chemotherapy on the ability of the baseline ADC value to predict tumor responses to therapy. Similar to previous studies, our results suggest that higher baseline ADC values are associated with poor response to chemotherapy [23,38,40], poorer clinical outcome [24] and that lower ADC values predict chemotherapy responsiveness. Yet unlike previous studies, our results indicate that the ADC values predict therapeutic outcome only for minimally treated patients. We found that the baseline ADC in patients who had received more than one prior therapy could not be reliably used for predicting treatment responses. Treatment effects on the tumor, such as increased fibrosis and scar tissue formation, may affect the ability of ADC values to be predictive of antitumor responses in heavily treated patients. It is well known that heavily-treated tumors are less likely to respond to antitumor therapies compared to less-treated or untreated tumors [41]. Therefore, the ADC value from DW-MRI studies may only be relevant for assessing patients who are not yet treated or are minimally treated. We are also further developing the image analysis techniques to enable more accurate quantification of the ADC values. More recently, we have refined the ADC estimation algorithm to more accurately account for the noise and lesion heterogeneity [41]. Overall, this pilot study provides compelling results about the role of DW-MRI as a restricted biomarker using MRI protocols that increase signal sensitivity and reduce potential motion artifacts for improved quality. A larger clinical study in patients with minimally treated liver metastases is warranted to further validate DW-MRI as a robust and predictive imaging biomarker.

Acknowledgments

Grant Support: NIH/NCI 5RO1 CA119046-05

The authors thank Merry Warner for assistance in study coordination and manuscript preparation.

References

1. Bammer R. Basic principles of diffusion-weighted imaging. Eur J Radiol. 2003; 45:169–184. [PubMed: 12595101]
2. Galons JP, Morse DL, Jennings DR, Gillies RJ. Diffusion-weighted MRI and response to anti-cancer therapies. Israel J Chem. 2003; 43:91–101.
3. Szafer A, Zhong J, Anderson AW, Gore JC. Diffusion-weighted imaging in tissues: theoretical models. NMR Biomed. 1995; 8:289–296. [PubMed: 8739267]
4. Reichardt W, Juettner E, Uhl M, Elverfeldt DV, Kontny U. Diffusion-weighted imaging as predictor of therapy response in an animal model of Ewing sarcoma. Invest Radiol. 2009; 44:298–303. [PubMed: 19346963]
5. Hamstra DA, Lee KC, Moffat BA, Chenevert TL, Rehemtulla A, Ross BD. Diffusion magnetic resonance imaging: an imaging treatment response biomarker to chemoradiotherapy in a mouse model of squamous cell cancer of the head and neck. Transl Oncol. 2008; 1:187–194. [PubMed: 19043529]
6. Jordan BF, Runquist M, Raghunand N, Baker A, Williams R, Kirkpatrick L, et al. Dynamic contrast-enhanced and diffusion MRI show rapid and dramatic changes in tumor microenvironment in response to inhibition of HIF-1alpha using PX-478. Neoplasia. 2005; 7:475–485. [PubMed: 15967100]
7. Lee KC, Sud S, Meyer CR, Moffat BA, Chenevert TL, Rehemtulla A, et al. An imaging biomarker of early treatment response in prostate cancer that has metastasized to the bone. Cancer Res. 2007; 67:3524–3528. [PubMed: 17440058]
8. Jennings D, Hatton BN, Guo J, Galons JP, Trouard TP, Raghunand N, et al. Early response of prostate carcinoma xenografts to docetaxel chemotherapy monitored with diffusion MRI. Neoplasia. 2002; 4:255–262. [PubMed: 11988845]
9. Hall DE, Moffat BA, Stojanovska J, Johnson TD, Li Z, Hamstra DA, et al. Therapeutic efficacy of DTI-015 using diffusion magnetic resonance imaging as an early surrogate marker. Clin Cancer Res. 2004; 10:7852–7859. [PubMed: 15585617]
10. Lee KC, Moffat BA, Schott AF, Layman R, Ellingsworth S, Juliar R, et al. Prospective early response imaging biomarker for neoadjuvant breast cancer chemotherapy. Clin Cancer Res. 2007; 13:443–450. [PubMed: 17255264]
11. Moffat BA, Chenevert TL, Lawrence TS, Meyer CR, Johnson TD, Dong Q, et al. Functional diffusion map: a noninvasive MRI biomarker for early stratification of clinical brain tumor response. Proc Natl Acad Sci USA. 2005; 102:5524–5529. [PubMed: 15805192]
12. Mardor Y, Pfeffer R, Spiegelmann R, Roth Y, Maier SE, Nissim O, et al. Early detection of response to radiation therapy in patients with brain malignancies using conventional and high b-value diffusion-weighted magnetic resonance imaging. J Clin Oncol. 2003; 21:1094–1100. [PubMed: 12637476]
13. Mardor Y, Roth Y, Lidar Z, Jonas T, Pfeffer R, Maier SE, et al. Monitoring response to convection-enhanced taxol delivery in brain tumor patients using diffusion-weighted magnetic resonance imaging. Cancer Res. 2001; 61:4971–4973. [PubMed: 11431326]
14. Sun YS, Zhang XP, Tang L, Ji JF, Gu J, Cai Y, et al. Locally advanced rectal carcinoma treated with preoperative chemotherapy and radiation therapy: preliminary analysis of diffusion-weighted MR imaging for early detection of tumor histopathologic downstaging. Radiology. 2010; 254:170–178. [PubMed: 20019139]
15. Hein PA, Kremser C, Judmaier W, Griebel J, Pfeffer KP, Kreczy A, et al. Diffusion-weighted magnetic resonance imaging for monitoring diffusion changes in rectal carcinoma during combined, preoperative chemoradiation: preliminary results of a prospective study. Eur J Radiol. 2003; 45:214–222. [PubMed: 12595106]
16. Kremser C, Judmaier W, Hein P, Griebel J, Lukas P, de Vries A. Preliminary results on the influence of chemoradiation on apparent diffusion coefficients of primary rectal carcinoma measured by magnetic resonance imaging. Strahlenther Onkol. 2003; 179:641–649. [PubMed: 14628131]

17. DeVries AF, Kremser C, Hein PA, Griebel J, Lukas P, de Vries A. Tumor microcirculation and diffusion predict therapy outcome for primary rectal carcinoma. Int J Radiat Oncol Biol Phys. 2003; 56:958–965. [PubMed: 12829130]

18. Oka K, Yakushiji T, Sato H, Hirai T, Yamashita Y, Mizuta H. The value of diffusion-weighted imaging for monitoring the chemotherapeutic response of osteosarcoma: a comparison between average apparent diffusion coefficient and minimum apparent diffusion coefficient. Skeletal Radiol. 2010; 39:141–146. [PubMed: 19924412]

19. Hayashida Y, Yakushiji T, Awai K, Katahira K, Nakayama Y, Shimomura O, et al. Monitoring therapeutic responses of primary bone tumors by diffusion-weighted image: Initial results. Eur Radiol. 2006; 16:2637–2643. [PubMed: 16909220]

20. Theilmann RJ, Borders R, Trouard TP, Xia G, Outwater E, Ranger-Moore J, et al. Changes in water mobility measured by diffusion MRI predict response of metastatic breast cancer to chemotherapy. Neoplasia. 2004; 6:831–837. [PubMed: 15720810]

21. Nilsen L, Fangberget A, Geier O, Olsen DR, Seierstad T. Diffusion-weighted magnetic resonance imaging for pretreatment prediction and monitoring of treatment response of patients with locally advanced breast cancer undergoing neoadjuvant chemotherapy. Acta Oncol. 2010; 49:354–360. [PubMed: 20397769]

22. Tozaki M, Oyama Y, Fukuma E. Preliminary study of early response to neoadjuvant chemotherapy after the first cycle in breast cancer: comparison of 1H magnetic resonance spectroscopy with diffusion magnetic resonance imaging. Jpn J Radiol. 2010; 28:101–109. [PubMed: 20182844]

23. Cui Y, Zhang XP, Sun YS, Tang L, Shen L. Apparent diffusion coefficient: potential imaging biomarker for prediction and early detection of response to chemotherapy in hepatic metastases. Radiology. 2008; 248:894–900. [PubMed: 18710982]

24. Tam HH, Collins DJ, Brown G, Chau I, Cunningham D, Leach MO, Koh D-M. The role of pre-treatment diffusion-weighted MRI in predicting long-term outcome of colorectal liver metastasis. Brit J Radiol. 2013; 86:20130281. [PubMed: 23995873]

25. Kele PG, van der Jagt EJ. Diffusion weighted imaging in the liver. World J Gastroenterol. 2010; 16:1567–1576. [PubMed: 20355235]

26. Padhani AR, Liu G, Koh DM, Chenevert TL, Thoeny HC, Takahara T, et al. Diffusion-weighted magnetic resonance imaging as a cancer biomarker: consensus and recommendations. Neoplasia. 2009; 11:102–125. [PubMed: 19186405]

27. Jha AK, Rodriguez JJ, Stephen RM, Stopeck AT. A clustering algorithm for liver lesion segmentation of diffusion-weighted MR images. IEEE Southwest Symp Image Analysis and Interpretation. 2010:93–96.

28. Jha AK, Kupinski MA, Rodriguez JJ, Stephen RM, Stopeck AT. ADC estimation of lesions in diffusion-weighted MR images: a maximum-likelihood approach. IEEE Southwest Symp Image Analysis and Interpretation. 2010:209–212.

29. Jha AK, Kupinski MA, Rodriguez JJ, Stephen RM, Stopeck AT. ADC estimation in multi-scan DWMRI. Digital Image Processing and Analysis, OSA. 2010:DTuB3-1–DTuB3-3.

30. Jha AK, Kupinski MA, Rodriguez JJ, Stephen RM, Stopeck AT. Task-based evaluation of segmentation algorithms for diffusion-weighted MRI without using a gold standard. Phys Med Biol. 2012; 57(13):4425–46. Corrigendum Phys Med Biol 2013, 58(1), 183. [PubMed: 22713231]

31. Jha, AK.; Rodriguez, JJ. A maximum-likelihood approach for ADC estimation of lesions in visceral organs. IEEE Southwest Symposium on Image Analysis and Interpretation; 2012; p. 21-24.

32. Jha, AK. MS thesis. Department of Electrical and Computer Engineering, University of Arizona; 2009. ADC Estimation in Diffusion-Weighted Images.

33. Haralick RM, Sternberg SR, Zhuang X. Image analysis using mathematical morphology. IEEE Transactions on Pattern Analysis and Machine Intelligence. 1987; PAMI-9:532–550. [PubMed: 21869411]

34. Vogel-Claussen J, Gimi B, Artemov D, Bhujwalla ZM. Diffusion-weighted and macromolecular contrast enhanced MRI of tumor response to antivascular therapy with ZD6126. Cancer Biol Ther. 2007; 6:1469–1475. [PubMed: 17881899]

35. Thoeny HC, De Keyzer F, Chen F, Vandecaveye V, Verbeken EK, Ahmed B, et al. Diffusion-weighted magnetic resonance imaging allows noninvasive in vivo monitoring of the effects of combretastatin a-4 phosphate after repeated administration. Neoplasia. 2005; 7:779–787. [PubMed: 16207480]

36. Tunariu N, d'Arey JA, Morgan VA, MGermuska M, Simpkin CG, Giles SL, et al. Assessment of variability of region of interest (ROI) delineation on diffusion weighted MRI (DW-MRI) using manual and semi-automated computer methods. Proc Intl Soc Mag Reson Med. 2010

37. Thoeny HC, Ross BD. Predicting and monitoring cancer treatment response with diffusion-weighted MRI. J Magn Reson Imaging. 2010; 32:2–16. [PubMed: 20575076]

38. Koh DM, Scurr E, Collins D, Kanber B, Norman A, Leach MO, et al. Predicting response of colorectal hepatic metastasis: value of pretreatment apparent diffusion coefficients. AJR Am J Roentgenol. 2007; 188:1001–1008. [PubMed: 17377036]

39. Dudeck O, Zeile M, Wybranski C, Schulmeiseter A, Fischbach F, Pech M, et al. Early prediction of anticancer effects with diffusion-weighted MR imaging in patients with colorectal liver metastases following selective internal radiotherapy. Eur Radiol. 2010; 20:2699–2706. [PubMed: 20563725]

40. Dzik-Jurasz A, Domenig C, George M, Wolber J, Padhani A, Brown G, et al. Diffusion MRI for prediction of response of rectal cancer to chemoradiation. Lancet. 2002; 360:307–308. [PubMed: 12147376]

41. Ma AT, Ma BB, Lei KI, Mo FK, Chan AT. Clinical predictors of response to cetuximab-chemotherapy in metastatic colorectal cancer. Hong Kong Med J. 2010; 16:207–212. [PubMed: 20519757]

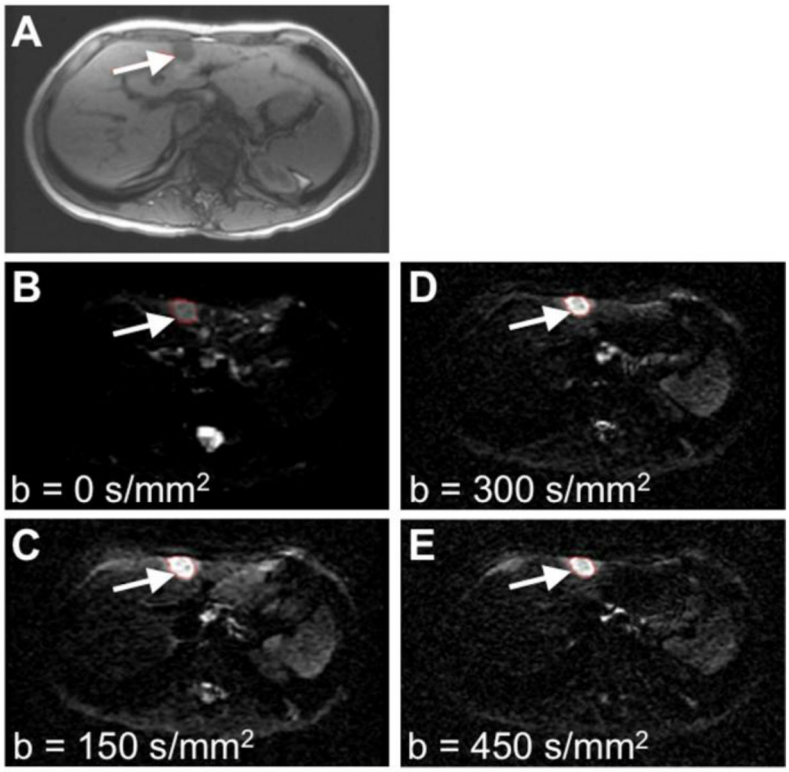

Figure 1.

Clinical MR images at baseline prior to treatment. A) A T1-weighted MR image was used to locate the tumor (arrow). B–E) Diffusion-weighted MR images with b=0, 150, 300 and 450 s/mm^2. Similar high quality images were obtained at other time points during the longitudinal study.

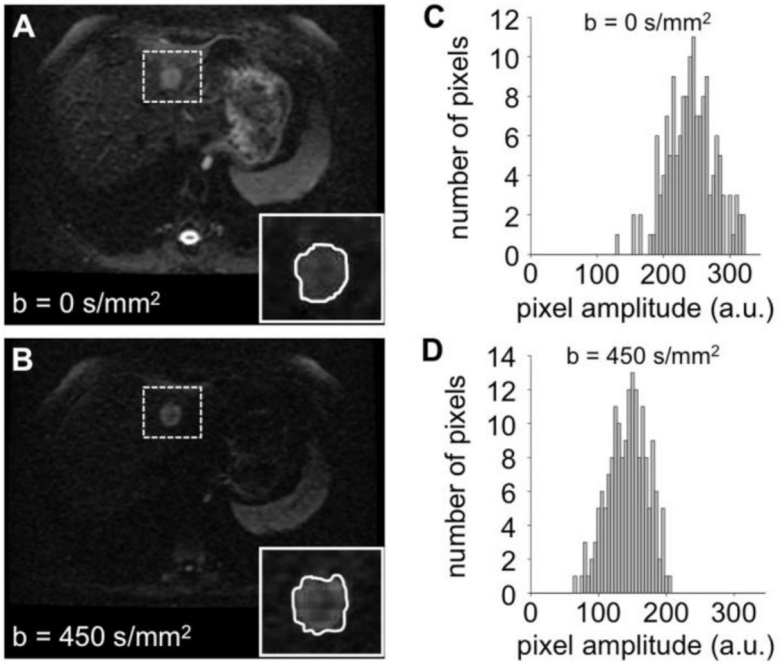

Figure 2.

Measurements of ADC values. A, B) DW-MR images of a liver lesion (highlighted with a dashed box) at two b values. The insets show the semi-automated ROI selected for the lesion in each image. C, D) Histograms of pixel amplitudes from the lesion ROIs showing pixel intensities within the region of interest. The lesion ADC value was calculated to be 1.19 $\mu m^2/ms$ +/− 0.2 $\mu m^2/ms$, using equation $I_{450} = I_0 e^{-bADC}$ with I_0 = average intensity at b=0 s/mm^2, I_{450} = average intensity at b=450 s/mm^2. The average signal intensities were computed at each b-value. The ADC value that maximized the probability of occurrence of the measured average signal intensities was then determined (28).

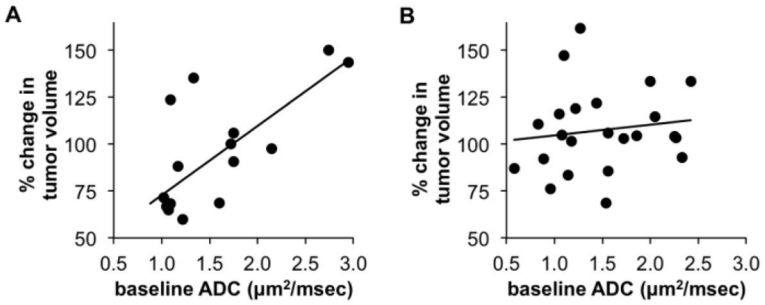

Figure 3.

Predictive ability of the baseline ADC value. A) The relative change in tumor size at day 39 was correlated with the baseline ADC value for minimally treated patients (n = 14 lesions, 8 patients). A fitted regression line showed a statistically significant relationship (p = 0.002). B) The same correlation was investigated for lesions in heavily treated patients (n = 23 lesions, 10 patients). The fitted regression line showed no statistically significant relationship (p = 0.29).

Table 1

Patient Demographics

Characteristic	
Age	Mean 52 yrs; Range: 30 – 82 yrs
Minimally Treated	8 (44%)
Heavily Treated	10 (55%)
Chemotherapy Regimens	
Taxane	4
Capecitabine	5
Chemotherapy Doublet	4
Other Chemotherapy Agents	5

Table 2

Comparison of the ADC values (in units of $\mu m^2/ms$) determined with different b-values

	Sample Size	Mean (SE)			p-values		
		b0–b150	b0–b300	b0–b450	b0–b150 vs. b0–b300	b0–b150 vs. b0–b450	b0–b300 vs. b0–b450
Baseline	19	2.67 (0.29)	1.46 (0.10)	1.44 (0.09)	<0.0001	<0.0001	0.951
Day 4	18	1.78 (0.20)	1.57 (0.10)	1.48 (0.08)	0.298	0.127	0.619
Day 11	19	2.16 (0.21)	1.57 (0.14)	1.43 (0.10)	0.003	<0.001	0.450
Day 39	19	2.09 (0.24)	1.62 (0.12)	1.48 (0.09)	0.038	0.022	0.808

Note: SE = standard error shown in parentheses

Table 3

Comparison of the ADC values (in units of $\mu m^2/ms$) of a Single Central Slice versus Multiple Slices (n = 5)

	Fully Automated	Fully Manual	Semi-Automated
	Mean (SE)	**Mean (SE)**	**Mean (SE)**
Single Central Slice	1.63 (0.14)	1.54 (0.13)	1.52 (0.17)
Multiple Slices	1.75 (0.14)	1.58 (0.13)	1.45 (0.17)
p-value	0.463	0.748	0.626

Table 4

Comparison of Baseline ADC Values

Treated	Number of Patients	Number of Lesions	ADC Mean ($\mu m^2/ms$)	ADC Median ($\mu m^2/ms$)	ADC Range ($\mu m^2/ms$)	P-Value
Minimally	8	14	1.58	1.30	0.88 – 2.95	0.686
Heavily	10	23	1.48	1.44	0.58 – 2.42	